EPJ Web of Conferences **201**, 09004 (2019) https://doi.org/10.1051/epjconf/201920109004
AYSS-2018

Outflows and particle acceleration in the accretion disks of young stars

Sergey Khaibrakhmanov[1,2,*] and *Alexander* Dudorov[2]

[1]Ural Federal University, Kourovka Astronomical Observatory, 51 Lenina str., Ekaterinburg 620000, Russia
[2]Chelyabinsk State University, Theoretical Physics Department, 129 Bratiev Kashirinykh str., Cheyabinsk 454001, Russia

Abstract. Magneto-gas-dynamic (MGD) outflows from the accretion disks of T Tauri stars with fossil large-scale magnetic field are investigated. We consider two mechanisms of the outflows: rise of the magnetic flux tubes (MFT) formed in the regions of efficient generation of the toroidal magnetic field in the disk due to Parker instability, and acceleration of particles in the current layer formed near the boundary between stellar magnetosphere and the accretion disk. Structure of the disk is calculated using our MGD model of the accretion disks. We simulate dynamics of the MFT in frame of slender flux tube approximation taking into account aerodynamic and turbulent drags, and radiative heat exchange with external gas. Particle acceleration in the current layer is investigated on the basis of Sweet-Parker model of magnetic reconnection. Our calculations show that the MFT can accelerate to velocities up to 50 km s^{-1} causing periodic outflows from the accretion disks. Estimations of the particle acceleration in the current layer are applied to interpret high-speed jets and X-rays observed in T Tauri stars with the accretion disks.

1 Introduction

Accretions disks form at the early stages of star formation. Typical sizes of the accretion disks of young T Tauri stars are 100 – 1000 au, masses range from 0.001 to 0.1 $M_\odot$, and mass accretion rates are $10^{-9} - 10^{-6}\,M_\odot\,\mathrm{yr}^{-1}$ (see review [1]). Temperature inside the disks ranges from several thousand K to 10 – 20 K. The accretion disks rotate with nearly Keplerian angular velocity $\Omega \propto r^{-3/2}$. Observations reveal outflows from the accretion disks of young stars. The outflows are divided into two groups: low-velocity outflows with $v = 10-50$ km s^{-1} and high-velocity well collimated jets with $v = 50 - 1000$ km s^{-1} (see review [2]).

Investigations of the polarization of dust thermal emission from the accretion disks of young stars have detected large-scale magnetic field with complex geometry in the disks [3]. Measurements of the magnetic field strength are still challenging, but there is indication that the magnetic field strength near the inner edge of the accretion disks may achieve ~ 1 kG [4]. This is comparable with the magnetic field strength of the T Tauri stars having $B_\star \sim 1-3$ kG at their surface. If magnetic fields of star and disk are oppositely directed, then current layer can form near the boundary of stellar magnetosphere.

*e-mail: khaibrakhmanov@csu.ru

Accretion with velocity v_r amplifies the initial poloidal magnetic field on the accretion time scale. Differential rotation with velocity v_φ generates toroidal magnetic field from the poloidal one on the rotation time scale. In the accretion disks of young stars $v_r \ll v_\varphi$, and intense toroidal magnetic field is generated in the regions, where the magnetic field is frozen in gas. The question is, what mechanisms hinder fast generation of the toroidal magnetic field? Parker has shown that the gas layer with planar magnetic field is unstable and tends to split into separate magnetic flux tubes (see book [5]). Magnetic flux tubes (MFT) float from the gas under the action of Archimedes force carrying away the excess of magnetic flux.

In this work, we develop our approach [6, 7] and simulate the dynamics of the MFT in the accretion disks of T Tauri stars (Section 2). We also consider particle acceleration in the current layer formed at the boundary of the stellar magnetosphere (Section 3).

2 Dynamics of the magnetic flux tubes

2.1 Model

Consider an accretion disk around young star with mass M. We use cylindrical coordinate system $(r,\ 0,\ z)$, where r is the radial distance from the star, z is the height above the equatorial plane of the disk. We assume that Parker instability leads to formation of the MFT out of the toroidal magnetic field B in the disk. The MFT has the form of rings with major radius r. In slender flux tube approximation, we investigate dynamics of unit length cylindrical MFT with radius a, density ρ, temperature T, velocity v and magnetic field strength B. Motion in z-direction under the action of buoyant and drag forces $f_{\rm d}$ is modelled. We consider turbulent drag inside the disk and aerodynamic drag above the disk. The accretion disk is characterized by density $\rho_{\rm e}$, pressure $P_{\rm e}$, temperature $T_{\rm e}$, magnetic field strength B_z, and scale height H.

Motion of the MFT is modelled by solving the system of differential equations (see [8])

$$\frac{dv}{dt} = (1-\rho_{\rm e}/\rho)\, g + f_d, \tag{1}$$

$$\frac{dz}{dt} = v, \tag{2}$$

$$\frac{d\rho}{dt} = \frac{h_{\rm c}\rho(\gamma-1)+\rho_e g v}{(\gamma-1)\rho\,(C_{\rm m}\rho - P_{\rm e}/\rho^2) - R_{\rm g}T/\mu - C_{\rm m}\rho}, \tag{3}$$

$$\frac{dT}{dt} = \frac{(1-\gamma)\mu}{R_{\rm g}}\frac{\rho_e g v\left(C_{\rm m}\rho - P_{\rm e}/\rho^2\right) + h_{\rm c}\left(R_{\rm g}T/\mu + C_{\rm m}\rho\right)}{(\gamma-1)\rho\,(C_{\rm m}\rho - P_{\rm e}/\rho^2) - R_{\rm g}T/\mu - C_{\rm m}\rho}, \tag{4}$$

$$a = a_0\,(\rho/\rho_0)^{-1/2}, \tag{5}$$

$$B = B_0(\rho/\rho_0), \tag{6}$$

where g is the vertical component of stellar gravity, $h_{\rm c}$ is the heating power per unit mass, γ is the adiabatic index, $C_{\rm m} = B_0^2/4\pi\rho_0^2$, $R_{\rm g}$ is the universal gas constant, $\mu = 2.3$ is the molecular weight of the gas, a_0, ρ_0 and B_0 are the initial radius, density and magnetic field strength of the MFT.

Equations (3) and (4) are derived from the first law of thermodynamics, equation of pressure balance taking into account the hydrostatic equilibrium of the disk. Equations (5) and (6) follow from MFT mass and magnetic flux conservation. Heating power $h_{\rm c}$ is determined in the diffusion approximation under the assumption that the heat exchange occurs due to radiative heat conductivity.

Radial structure of the disk is calculated using our MGD model of the accretion disks [9, 10]. Vertical structure of the disk is calculated from the equation of the hydrostatic

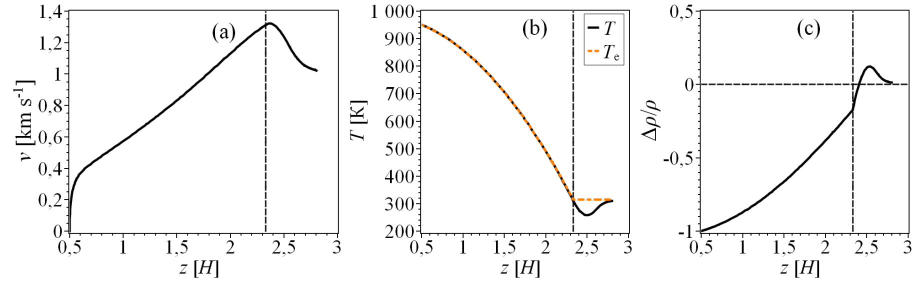

Figure 1. Dependence of the MFT velocity (panel a), temperature inside and outside the MFT (panel b) and relative densities difference (panel c) on coordinate z in run with $a_0 = 0.1\,H, \beta_0 = 1$ and $z_0 = 0.5\,H$. Vertical dashed lines indicate the surface of the disk $z_s = 2.33\,H$.

equilibrium assuming that the disk is polytropic with polytropic index $n = 2.5$. Temperature of the atmosphere above the disk is constant $T_{\rm atm}$.

2.2 Results

We consider T Tauri star with $M = 1\,M_\odot$ and the accretion disk with accretion rate $\dot{M} = 10^{-8}\,M_\odot\,{\rm yr}^{-1}$, turbulence parameter $\alpha = 0.01$. Simulations are performed for $r = 0.8$ au, where $H = 0.045$ au, $\rho_e(z = 0) = 8.4\times10^{-10}\,{\rm g\,cm^{-3}}$, $T_e(z = 0) = 980$ K, $T_{\rm atm} = 315$ K, $B_z = 0.16$ G. We present results of the simulations for the following parameters: initial plasma beta $\beta_0 = [0.01, 0.1, 1]$, radius $a_0 = [0.001,\ 0.5]\ H$, initial height above the midplane $z_0 = [0.1,\ 2]\ H$. We assume that initially the MFT is in thermal equilibrium with the ambient gas, $T_0 = T_e$. Initial density ρ_0 of the MFT is calculated from the pressure equilibrium $P_0 = P_e$.

Dynamical equations (1, 2, 3, 4) are solved using the fourth order Runge-Kutta method with automatic time step control and relative accuracy 10^{-6}.

In Figure 1, we plot dependence of the MFT velocity (panel a), temperature (panel b) and relative densities difference $\Delta\rho/\rho = (\rho - \rho_e)/\rho$ (panel c) on coordinate z in run with $a_0 = 0.1\,H$, $\beta_0 = 1$ and $z_0 = 0.5\,H$. Figure 1 shows that the MFT accelerates inside the disk and reaches the surface of the disk, $z_s = 2.33\,H$, with velocity of $\approx 1.3\,{\rm km\,s^{-1}}$ over time $t \simeq 5\Omega^{-1}$. After that, the MFT decelerates, and ultimately it acquires terminal speed $v \approx 1\,{\rm km\,s^{-1}}$.

During motion inside the disk, temperatures inside and outside the MFT are practically equal to each other due to efficient radiative heat exchange (see Figure 1b). Above the disk, $z \simeq 2.5\,H$, the MFT cools down by $\sim$ 100 K compared to the ambient gas. After that, the temperature difference decreases to zero at higher altitudes.

Figure 1c shows that inside the disk the densities difference is negative and decreases during the MFT rise. Above the disk, the densities difference becomes positive, therefore the MFT loses buoyancy and decelerates. Ultimately $\Delta\rho$ approaches zero, the buoyant force diminishes, and the MFT moves further by inertia.

In Figure 2, we plot the time of the MFT rise to the surface of the disk, $t_{\rm rise}$, as a function of initial plasma beta and radius. Time scale of the toroidal magnetic field generation (see [9])

$$t_{\rm gen} = 13\,\Omega^{-1}(B/B_z), \tag{7}$$

is also depicted. Figure 2 shows that $t_{\rm rise}$ increases with β_0. For example, the MFT with $a_0 = 0.1\,H$ and $\beta_0 = 1$ rises to the surface of the disk within $t = 0.8\,P_{\rm orb}$, while the rise

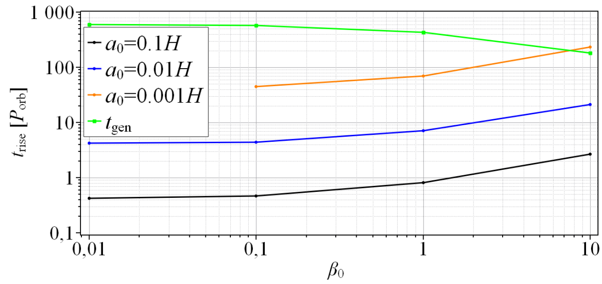

Figure 2. Dependence of the time of the MFT rise to the surface of the disk on initial plasma beta and radius of the MFT. Black line: $a_0 = 0.1\,H$, blue line: $a_0 = 0.01\,H$, orange line: $a_0 = 0.001\,H$. Green line shows time scale of the magnetic field generation. Time is measured in rotation periods $P_{\rm orb}$.

time for the MFT with $\beta_0 = 10$ is of $\sim 3\,P_{\rm orb}$, where $P_{\rm orb} = 2\pi/\Omega$. According to Figure 2, rise time scales as $\propto a_0^{-1}$. Our simuations show that $v \propto a_0$, correspondingly. The MFT with larger initial radius float faster, as they have larger volume and, correspondingly, are more buoyant. The MFT with $a_0 = 1\,H$, $\beta_0 = 0.1$ can accelerate to $v = 50\,{\rm km\,s^{-1}}$ that is comparable with velocity of observed outflows from the accretion disks [8]. Rise of the MFT solves the problem of the toroidal magnetic field growth stabilization in the disk.

3 Current layer

According to theory of fossil magnetic field (see review of the theory in [11, 12]), stellar magnetic field, after separation from the external field, can be directed oppositely to the magnetic field of the accretion disk. Therefore, current layer can form near the boundary of stellar magnetosphere.

Let the current layer be a cylindrical shell with radius $r_{\rm m}$ and height $H_{\rm CL}$, where $r_{\rm m}$ is the radius of stellar magnetosphere. We estimate the luminosity of the current layer as the magnetic energy entering the layer per unit of time

$$L_{\rm CL} = v_r \cdot (B_z^2/8\pi) \cdot 2\pi r_{\rm m} \cdot 2H_{\rm CL}. \tag{8}$$

Taking into account the definition of mass accretion rate $\dot{M} = 2\pi r v_r (2\rho_{\rm e} H)$, we derive

$$L_{\rm CL} = \dot{M} v_{\rm a}^2/2, \tag{9}$$

where $v_{\rm a}$ is the Alfvén speed inside the current layer.

Reconnection of the magnetic field lines inside the current layer leads to particle acceleration in z-direction. According to Sweet-Parker model of reconnection, outflow velocity equals to $v_{\rm a}$ [13]. We plot dependence $v_{\rm a}(z)$ in Figure 3a. For the considered parameters $r_{\rm m} = 0.03$ au, $\rho_{\rm e} = 4.7\times10^{-7}\,{\rm g\,cm^{-3}}$, $H = 0.0006$ au, $B_z = 170$ G. Alfvén velocity increases with z, when the density falls down. If the current layer forms at $H_{\rm CL} = 4-5\,H$, then the magnetic reconnection can drive outflows with velocity of $\sim 100\,{\rm km\,s^{-1}}$.

If we assume that the current layer radiates as a black body, then we can estimate the temperature inside it,

$$T = \left(v_r B_z^2/8\pi\sigma_{\rm sb}\right)^{1/4}, \tag{10}$$

where $\sigma_{\rm sb}$ is Stephan-Boltzmann constant. We plot this dependence in Figure 3b. This estimation shows that the current layer at $H_{\rm CL} = 6\,H$ can be heated up to $(1-2)\cdot10^4$ K, and therefore produce UV radiation. If the current layer forms at higher altitudes, then it can be the source of X-rays.

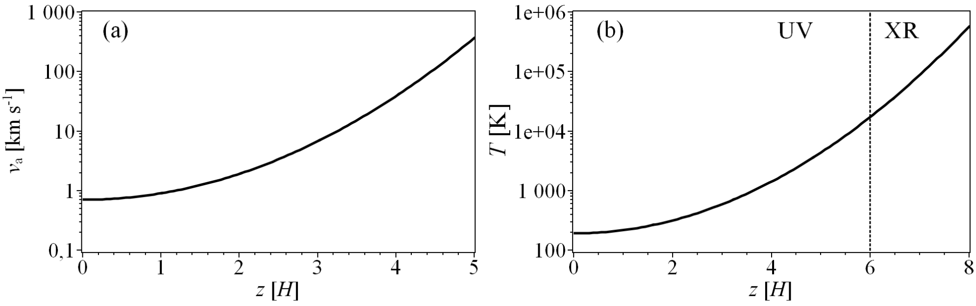

Figure 3. Panel a: dependence of the Alfvén speed on the height of the current layer. Panel b: dependence of the temperature of the current layer on its height.

4 Conclusion

Our calculations show that the MFT formed in the regions of efficient magnetic field generation rise with speeds up to 50 km s^{-1} from the accretion disks of young stars. We propose that the rising MFT can cause periodic outflows, as well as contribute to infrared variability of the accretion disks [8].

We assume that the current layer forms at the boundary of the magnetosphere between the star and disk. Reconnection of stellar and disk's magnetic field in the current layer can drive jets with velocity $\sim$ 100 km s^{-1} and produce observed UV and X-ray radiation.

Acknowledgements. We thank anonymous referee for useful comments. The work is supported by Russian Foundation for Basic Research (project 18-02-01067) and by the Ministry of Science and High Education (the basic part of the State assignment, RK no. AAAA-A17-117030310283-7).

References

[1] J.P. Williams, L.A. Cieza, ARA&A **49**, 67 (2011), 1103.0556
[2] A. Frank, T.P. Ray, S. Cabrit, P. Hartigan, H.G. Arce, F. Bacciotti, J. Bally, M. Benisty, J. Eislöffel, M. Güdel et al., Protostars and Planets VI pp. 451–474 (2014), 1402.3553
[3] D. Li, C.M. Telesco, H. Zhang, C.M. Wright, E. Pantin, P.J. Barnes, C. Packham, MNRAS **473**, 1427 (2018), 1708.08026
[4] J.F. Donati, F. Paletou, J. Bouvier, J. Ferreira, Nature **438**, 466 (2005)
[5] E.N. Parker, *Cosmical magnetic fields: Their origin and their activity* (1979)
[6] A.E. Dudorov, S.A. Khaibrakhmanov, A&AT **29**, 429 (2016)
[7] S.A. Khaibrakhmanov, A.E. Dudorov, PEPAN Letters **14**, 882 (2017)
[8] S. Khaibrakhmanov, A. Dudorov, A. Sobolev, RAA **18**, 090 (2018), 1712.09094
[9] A.E. Dudorov, S.A. Khaibrakhmanov, Ap&SS **352**, 103 (2014), 1403.5513
[10] S.A. Khaibrakhmanov, A.E. Dudorov, S.Y. Parfenov, A.M. Sobolev, MNRAS **464**, 586 (2017), 1609.03969
[11] A.E. Dudorov, ARep **39**, 790 (1995)
[12] A.E. Dudorov, S.A. Khaibrakhmanov, Adv Space Res **55**, 843 (2015), 1406.4663
[13] E.N. Parker, J Geophys Res **62**, 509 (1957)